Biosensors and Bioelectronics 24 (2009) 1223–1229

Contents lists available at ScienceDirect

Biosensors and Bioelectronics

journal homepage: www.elsevier.com/locate/bios

Novel poly-silicon nanowire field effect transistor for biosensing application

Cheng-Yun Hsiao [a], Chih-Heng Lin [a], Cheng-Hsiung Hung [b], Chun-Jung Su [b], Yen-Ren Lo [a], Cheng-Che Lee [a], Horng-Chin Lin [b], Fu-Hsiang Ko [c], Tiao-Yuan Huang [b], Yuh-Shyong Yang [a,d,*]

[a] Institute of Biological Science and Technology, National Chiao Tung University, Hsinchu 300, Taiwan
[b] Institute of Electronics, National Chiao Tung University, Hsinchu 300, Taiwan
[c] Institute of Nanotechnology, National Chiao Tung University, Hsinchu 300, Taiwan
[d] Instrument Technology Research Center and National Nano Device Laboratories, NARL, Hsinchu 300, Taiwan

ARTICLE INFO

Article history:
Received 14 April 2008
Received in revised form 11 July 2008
Accepted 14 July 2008
Available online 26 July 2008

Keywords:
Nanowire field effect transistor
Biosensing
Semiconductor device

ABSTRACT

A simple and low-cost method to fabricate poly-silicon nanowire field effect transistor (poly-Si NW FET) for biosensing application was demonstrated. The poly-silicon nanowire (poly-Si NW) channel was fabricated by employing the poly-silicon (poly-Si) sidewall spacer technique, which approach was comparable with current commercial semiconductor process and forsaken expensive E-beam lithography tools. The electronic properties of the poly-Si NW FET in aqueous solution were found to be similar to those of single-crystal silicon nanowire field effect transistors reported in the literature. A model biotin and avidin/streptavidin sensing system was used to demonstrate the biosensing capacity of poly-Si NW FET. The changes of I_D–V_G curves were consistent with an n-type FET affected by a nearby negatively (streptavidin) and positively (avidin) charged molecules, respectively. Specific electric changes were observed for streptavidin and avidin sensing when nanowire surface of poly-Si NW FET was modified with biotin and streptavidin at sub pM to nM range could be distinguished. With its excellent electric properties and the potential for mass commercial production, poly-Si NW FET can be a very useful transducer for a variety of biosensing applications.

1. Introduction

The development of highly sensitive biological sensors could impact significantly the areas of genomics, proteomics, biomedical diagnostics, and drug discovery (Hahm and Lieber, 2004). In recent years, the applications of semiconductor nanodevices in life sciences have attracted a lot of attention (Besteman et al., 2003; Cui et al., 2001; Hahm and Lieber, 2004; Li et al., 2005; Patolsky et al., 2004, 2006c; Star et al., 2006; Wang et al., 2005). Due to the large surface-to-volume ratio (Chen et al., 2007), silicon nanowire field effect transistor (Si NW FET) gives extraordinary sensitivity as transducer for biosensing when compared to other transducer reported in the literatures (Campagnolo et al., 2004; Hirotsugu et al., 2007; Wu et al., 2001; Zhang and Heller, 2005; Zheng et al., 2005). This is because the depletion or accumulation of charge carriers, which may be produced by specific binding of a charged biological macromolecule on the surface, can affect the entire cross-sectional conduction pathway of Si NW FET (Patolsky et al., 2006b). The function of single-crystal silicon nanowire (single-Si NW) as a Bio FET transistor (single-Si NW FET) has been demonstrated (Cui et al., 2001). It has been shown that single-Si NW FET can serve as a transducer for label free, direct, highly sensitive, real-time and multi-detection of a variety of chemicals and biological species such as drugs, virus, and cancer marker (Cui et al., 2001; Hahm and Lieber, 2004; Patolsky et al., 2004, 2006a; Wang et al., 2005; Zheng et al., 2005).

Although single-Si NW FETs are shown to be very powerful tools for biomedical application, the availability of the device seriously limits its future applications. Si NW FETs can be prepared by either 'top-down' or 'bottom-up' lithography approaches (Lin et al., 2005). The top-down approaches typically employ advanced optical or E-beam lithography tools to generate the NW patterns (Lee et al., 2007; Li et al., 2004). Although compatible with mass-production, the use of advanced lithography tools with nanometer size resolution is costly. The bottom-up approaches usually employ metal-catalytic growth for preparation of NWs (Cui et al., 2001; Duan et al., 2002, 2003; McAlpine et al., 2003). The later approaches, however, suffer seriously from the difficulty in precisely positioning the device location. Metal contamination and control of structural parameters are additional issues that need to be addressed for practical manufacturing. Available protocol for Si NW FET fabrication at present time (Patolsky et al., 2006d) indicates that Si NW FET is difficult to be prepared and is unlikely to be developed into a com-

* Corresponding author at: Institute of Biological Science and Technology, National Chiao Tung University, Hsinchu 300, Taiwan. Fax: +886 3 5729288.
E-mail address: ysyang@faculty.nctu.edu.tw (Y.-S. Yang).

0956-5663/$ – see front matter © 2008 Elsevier B.V. All rights reserved.
doi:10.1016/j.bios.2008.07.032

mercial scale production in the future. How to quickly fabricate a large amount of devices, control the electrical properties and down the cost to a reasonable range will be an important issue for using Si NW FET in biomedical applications.

A new method for fabrication of thin-film transistors with poly-silicon nanowire (poly-Si NW) channels has been proposed by us (Lin et al., 2005). Throughout the fabrication, no expensive lithography tools are needed for definition of nano-scale patterns. The fabricated devices exhibit good performance (Lin and Su, 2007; Su et al., 2006, 2007), indicating that the proposed method, albeit low-cost and simple, is potentially suitable for future practical manufacturing. Recently, the poly-silicon nanowire field effect transistor (poly-Si NW FET) has been shown to possess excellent electric properties in aqueous solution (Lin et al., 2007). Here, we demonstrate that the new transistors can indeed be developed into a sensitive and specific biological sensor. To illustrate the potential biological sensing application of the novel poly-Si NW FET, the well-known biotin–avidin/streptavidin interaction as model system was used. The result suggests that the device can serve as a transducer for biosensor for future biomedical application.

2. Materials and methods

2.1. Materials

Biotin 3-sulfo-*N*-hydroxysuccinimide ester sodium salt (biotin), (3-amonopropyl)triethoxysilane (APTES), mouse IgG, anti-mouse IgG (whole molecule)-gold, Tween 20, sodium cyanoborohydride ($NaBH_3CN$), ethanolamine and streptavidin were purchased from Sigma–Aldrich (USA). The avidin and 25% glutaraldehyde in aqueous solution were purchased from Fluka (USA). Sodium chloride, sodium phosphate monobasic and sodium phosphate dibasic were purchased from J.T. Backer (USA). Phosphate buffered solution (PBS) was prepared in deionized water and its pH was adjusted to 7.4. All reagent solutions were prepared with deionized water (resistance of water was 18.2 MΩ cm) from an ultra-pure water system (Barnstead).

2.2. Preparation of poly-Si NW FET

Poly-Si NW FETs were fabricated at the National Nano Device Laboratories (Hsinchu, Taiwan) according to procedures previously reported (Lin et al., 2005) with modifications to reduce their current leakage in aqueous solution. The key device fabrication steps are illustrated in Fig. 1. A bottom gate configuration was employed using 6-in. p-type Si (1 0 0) wafers as the starting materials and, for simplicity, as the gate electrode (Fig. 1(a)). The bottom gate could be used to adjust the channel potential, thus controlling the devices switching behavior. A gate dielectric was formed on a Si substrate by capping with a 100 nm wet-oxide layer and a 50 nm nitride layer. Poly-Si NW FETs without the nitride layer were also prepared to investigate the function of nitride as insulator to reduce current leakage when operated in aqueous solution. Then, a TEOS-dummy gate was formed (Fig. 1(b)) on the substrate and a 100 nm a-Si layer was deposited by low-pressure (LPCVD) (Fig. 1(c)). An annealing step was performed at 600 °C in nitrogen ambient for 24 h to transform the a-Si into poly-Si. Subsequently, source/drain (S/D) implant was performed (Fig. 1(d)). Note that the implant energy was kept low so that most implanted dopants (phosphorus) were located near the top surface of the Si layer. S/D photoresist patterns were then formed on the substrate by a standard lithography step. A reactive plasma etch step was subsequently used to remove the poly-Si layer. It should be noted that the sidewall Si channels were formed in this step in a self-aligned manner (Fig. 1(e)). Note that the implanted dopants in places other than S/D regions were removed during the etch step due to the shallow project range just mentioned. Afterwards, all devices were then deposited 300-nm thick TEOS oxide by LPCVD as the passivation layer and the S/D dopants were activated by an annealing treatment. The fabrication was completed after channel exposure and the formation of metal pads using lift-off methods. Top view of the fabricated device is shown in Fig. 1(f).

2.3. Electrical measurements

The gate potential and source/drain bias voltage were controlled with chip analyzer (Agilent 4156A or Keithley 4200A). In the general I_D–V_G curve measurement parameters, the drain current (I_D) was measured at constant bias voltage (V_D = 0.5 V) while sweeping the gate potential (V_G) from −2 to 10 V. In the general I_D–V_D curve measurement parameters, the V_G was measured at several constant bias voltage (from 0 to 5 V, ΔV = 1 V) while sweeping the V_D from 0 to 1 V. In the biosensing measurement parameters, the drain current was measured at constant bias voltage (V_D = 0.5 or 1 V) while sweeping the V_G from −1 to 10 V. To ensure that the device was in the same initial state, we performed a sweep started at −1 V bias. When comparing I_D–V_G curve behavior to those of control experiments, we noted that the biosensing tests gave the current shift at the same bias conduction.

2.4. Immobilization of biomolecules on poly-silicon

Immobilization of biotin on poly-Si NW surface was prepared by a two-step procedure. The poly-Si NW FETs were first washed by ethanol solution to remove contaminants, and then immersed in 2% APTES ethanol solution for 30 min, washed with pure ethanol, and heated at 120 °C for 10 min to remove surplus ethanol. Finally, sulfo-NHS–biotin (1 mg/ml) in ddwater was used to react with the APTES-modified device for 3 h. The un-reacted sulfo-NHS–biotin was removed with ddwater.

To confirm the functionalization of poly-Si NW with APTES as described above, anti-mouse IgG labeled with 5 nm Au nanoparticles were used as reporter protein in a separate experiment to show the successful protein immobilization on poly-Si NW. The poly-Si NW FETs were washed by ethanol solution to remove contaminants. Mouse IgG was immobilized on the poly-Si NW FET by a three-step procedure. First, the poly-Si NW FETs were immersed with a 2% APTES ethanol solution for 30 min, washed with pure ethanol, and heated at 120 °C for 15 min to remove surplus ethanol. Second, 2.5% glutaraldehyde in PBS buffer that contained 4 mM sodium cyanoborohydride were mixed with the devices for 1.5 h and washed with PBS buffer. Finally, mouse IgG (50 μg/ml) in PBS buffer that contain 4 mM sodium cyanoborohydride was coupled to the surface of nanowire for 9 h. The un-reacted aldehyde groups were blocked by ethanolamine and washed with PBS buffer. The mouse IgG immobilized poly-Si NW was then exposed to a solution of anti-mouse IgG gold (50 μg/ml) that contain 1% Tween 20 conjugate. The following processes were used for the preparation of poly-Si NW pattern to establish the procedure for molecular immobilization on poly-Si NW FET described above. A thermal oxide of 100 nm was first grown on a silicon wafer. Then a 90-nm thick amorphous silicon film was deposited on the wafer using a low-pressure chemical vapor deposition system. The film was then transformed into polycrystalline via an annealing step performed at 600 °C in nitrogen ambient. The SiNW channels were patterned simultaneously using E-beam lithography and subsequent plasma dry-etch step.

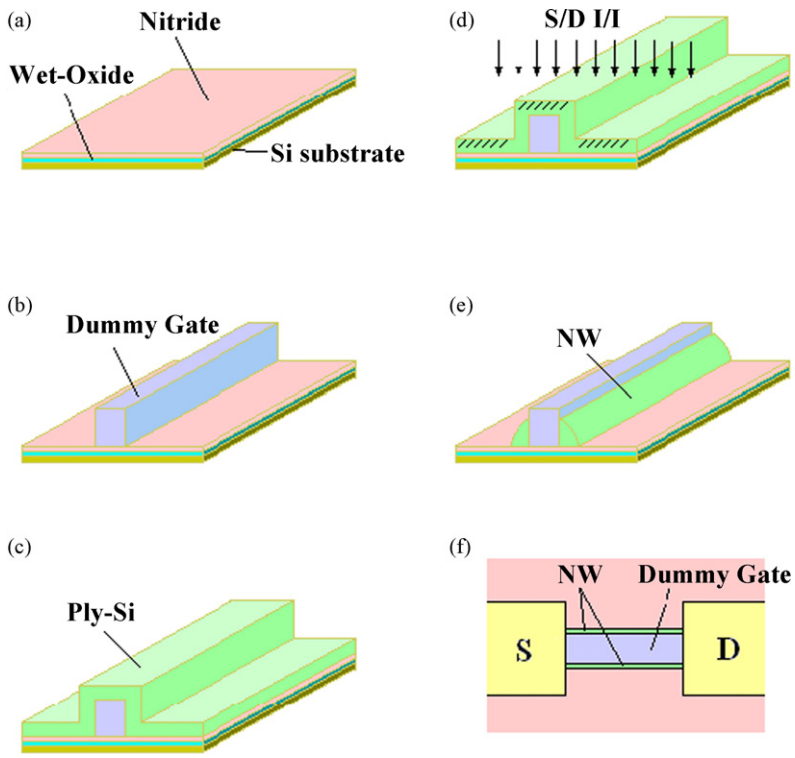

Fig. 1. Schematic diagram for the fabrication of poly-Si NW FET. (a) A bottom gate configuration was employed using 6-in. Si wafers capped with a 100 nm wet-oxide and 50 nm nitride layer as the starting materials and the gate electrode. (b) TEOS-dummy gate was formed on a Si substrate. The two insulator layers served as the gate dielectric. (c) A 100 nm a-Si layer was deposited by low-pressure (LPCVD) and the a-Si was transformed into poly-Si. (d) Source/drain (S/D) implant was performed. (e) The sidewall Si channels were formed in a self-aligned manner. (f) Top view of the fabricated device structure.

2.5. Scanning electron microscopy (SEM)

The samples (poly-Si NW FETs) were dried in 37 °C oven and then coated with 2 nm of Pt using a thermal evaporator (JFC-1600, JEOL, Japan). Scanning electron micrographs were obtained at 5, 10 and 15 kV, respectively (JSM-6700F, JEOL, Japan).

2.6. Interaction of biotin and avidin/streptavidin on poly-Si NW FET

Interaction between biotin and avidin/streptavidin on poly-Si NW FET was followed by measuring the change of I_D–V_G curve (as described in Section 2.3). After the stabilized base I_D–V_G curve was obtained in PBS buffer (10 mM, pH 7.4), PBS buffer solution contained mouse IgG (6 pM as negative control) was injected into the channel to obtain a similar stabilized base line curve to show that non-specific protein interaction was not observed. The device was washed by PBS buffer and a solution of streptavidin (16.7 pM) in PBS buffer was injected to obtain I_D–V_G curve represented poly-Si NW FET response from biotin–streptavidin interaction. The device was washed by PBS to regain the base line I_D–V_G curve. Similar procedures were followed to obtain I_D–V_G curve for biotin/avidin (1.48 nM) interaction. A control experiment using poly-Si NW FET without any surface modification was also performed to show that non-specific interaction was not observed between avidin/streptavidin and the naked poly-Si NW FET. The continuous fluidic transport was maintained by automatic syringe pump (KDS 270, KD Scientific, USA) with a microchannel run through poly-Si NW FET sensing surface.

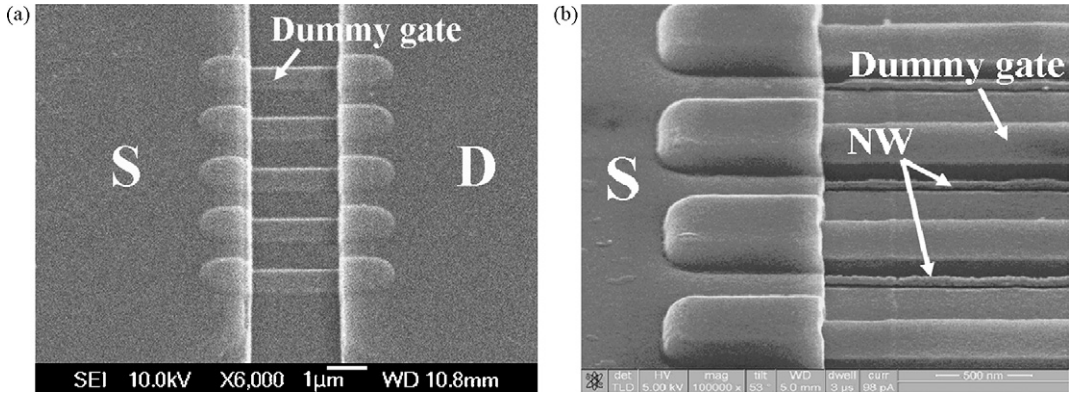

Fig. 2. SEM images of poly-Si NW FET. (a) SEM top view image of a parallel array of NW devices. The white arrow highlights the position of a dummy gate. (b) SEM side view of the device. The white arrow highlights the position of Si NWs and dummy gate.

3. Results and discussion

3.1. Device layout and electrical characterization of poly-Si NW FET

Poly-Si NW FET was prepared as outlined in Fig. 1, and the SEM images of silicon nanowire device array are shown in Fig. 2. In Fig. 2(a), the SEM image (6000×) shows five dummy gates (2 μm in length) between source and drain electrodes. The electrodes were passivated with silicon oxide to prevent the occurrence of leakage current between two electrodes when the device was used in aqueous environment. The SEM images of nanowires beside the dummy gates are shown in Fig. 2(b) with higher magnification power (100,000×). This poly-Si NW FET image was taken from one side to show the nanowire produced following spacer technique and the nanowire on the other side was hidden by the dummy gate and cannot be seen in Fig. 2(b). According to the fabrication process outlined in Fig. 1, 2 nanowires were produced with 1 dummy gate and thus poly-Si NW FET shown in Fig. 1(a) contained 10 nanowires. In our process, we were able to produce poly-Si NW FET containing 2–10 nanowires (i.e., with 1–5 dummy gates) with high efficiency, high-performance properties and reproducibility. This approach was comparable with current commercial semiconductor process and forsaken expensive E-beam lithography tools to fabricate Si NW channel. There is great potential that the proposed poly-Si NW FET can be obtained commercially in the future for biosensing and biomedical application.

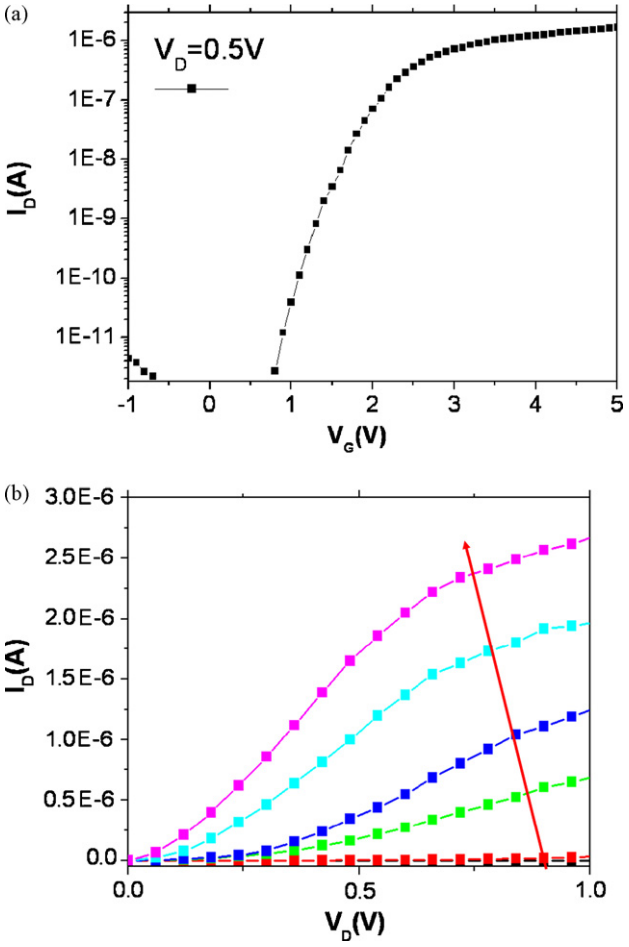

Fig. 3. Electric property of poly-Si NW FET. (a) I_D–V_G curve illustrating n-type behavior of a poly-Si NW FET. The electric property was performed at V_D = 0.5 V. (b) The I_D–V_D curves for varying V_G from 0 to 5 V at ΔV = 1 V. The red arrow highlights the direction from low to high V_G values. (For interpretation of the references to color in this figure legend, the reader is referred to the web version of the article.)

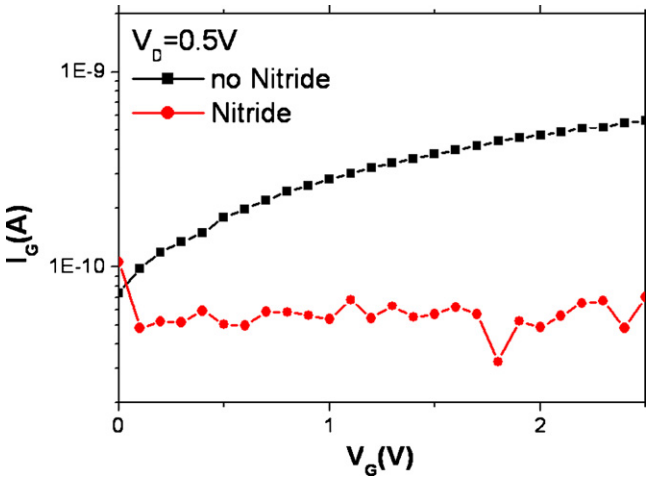

Fig. 4. Effect of nitride treatment on the gate leakage current of poly-Si NW FET. The I_G–V_G curves were obtained in distilled water at V_D = 0.5 V. The relationship between back-gate current (I_G) and back-gate voltage (V_G) is shown for poly-Si NW FET with (red circle) or without (black square) a nitride layer between back-gate and source/drain electrodes. (For interpretation of the references to color in this figure legend, the reader is referred to the web version of the article.)

Typical characteristics of the poly-Si NW FET at room temperature are shown in Fig. 3. The I_D versus V_G (from −1 to 5 V) output characteristics with the constant V_D (0.5 V) exhibited excellent semiconductor FET characteristics, illustrating n-type behavior. A good device performance with high on/off current ratio (around six orders) and reasonable subthreshold swing (250 mV/dec) was achieved (Fig. 3(a)). The I_D versus V_D output characteristics of a representative poly-Si NW FET are shown in Fig. 3(b) for V_G varying from 0 to 5 V with 1 V per step. The measured I_D–V_D characteristics showed well-saturated behavior with back-gate controlled. The electrical characterization verified that this fabrication approach produced high-performance poly-Si NW FET devices.

Another important issue for the preparation of highly sensitive FET devices for biosensing is to reduce the leakage current in aqueous solution between gate and source/drain electrode. In previous research, we demonstrated that a passivation layer over the source/drain electrode greatly suppresses the liquid-gate leakage of a CNT FET device (Lu et al., 2006). In order to simply set up the microfluidic channel for biosensing, we designed the back-gate to replace the liquid-gate in this experiment and a nitride layer was designed in between the back-gate and source/drain electrodes as shown in Fig. 1. To demonstrate the function of the nitride layer for the reduction of the leakage current between back-gate and source/drain electrode in aqueous solution, both poly-Si NW FETs with and without a nitride layer were prepared (Fig. 1(a)) and their I_G–V_G curves are shown in Fig. 4. In the absence of nitride layer, the gate current (I_G) increased with the increase of V_G. However, when the nitride layer was used to separate the silicon layer, the leakage current of I_G was kept under 1×10^{-10} A even when V_G was increased from 0 to 2.5 V (Fig. 4). Our results indicate that the presence of a nitride layer can keep the gate leakage current in low magnitude and is useful for biosensing application in aqueous solution, which is especially important when highly sensitive transducer is required.

3.2. Poly-Si NW surface modification and verification

To confirm the functionalization of poly-Si NW FET with APTES, anti-mouse IgG labeled with 5 nm Au nanoparticles were immo-

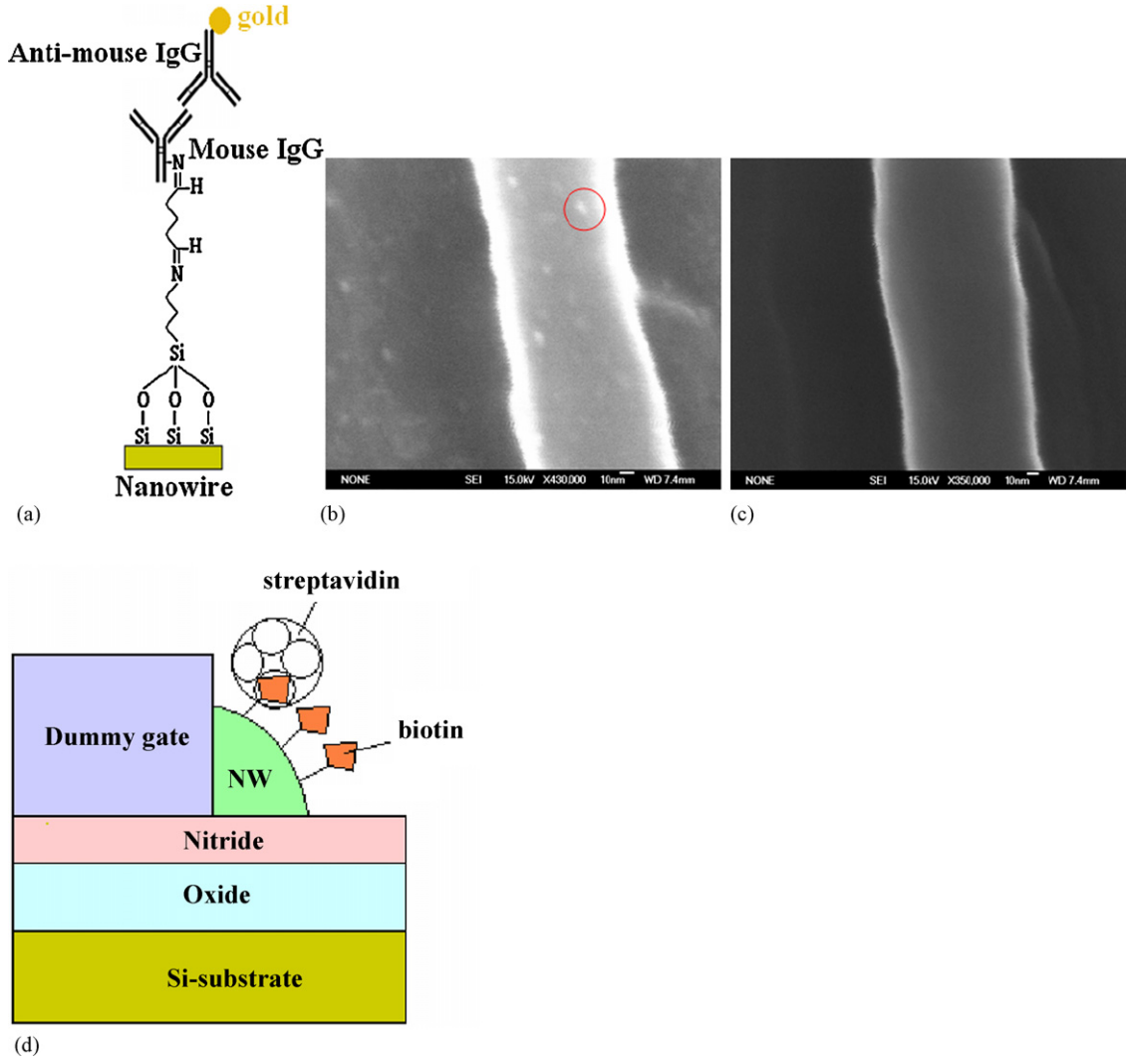

Fig. 5. Surface functionalization on poly-Si NW. (a) Schematic diagram of antibodies attach to APTES-modified surface. (b) SEM image of mouse IgG functionalized poly-Si NW following with 5 nm gold labeled anti-mouse IgG addition. (c) SEM image of poly-Si NW without surface functionalization. (d) Illustration of biotin-modified poly-Si NW FET device.

bilized onto poly-Si NW (Fig. 5(a)) following cross-linking with glutaraldehyde. Subsequent SEM image (Fig. 5(b)) confirmed that anti-mouse IgG did indeed bind strongly to the immobilized mouse IgG on the poly-Si NW. The SEM image of the control experiment (Fig. 5(c)), in which the poly-Si NW was without any prior treatment, shows free of anti-mouse IgG binding. In our model study for biosensing, biotin was immobilized on poly-Si NW FET as diagramed in Fig. 5(d). The proposed interaction of biotin with streptavidin is also shown.

3.3. *Electric responses from the interaction of biotin and streptavidin/avidin on poly-Si NW FET*

Sensitivity and specificity of poly-Si NW FET as transducer for biosensing were characterized using the well-known biotin–avidin/streptavidin model system as shown in Fig. 6. The biotinylated device was first shown to specifically bind to streptavidin and avidin (Fig. 6(a) and (b)). The addition of streptavidin, which p*I* is around 10, resulted in a current decrease due to the protein's net negative charge in pH 7.4 solution, whereas the addition of mouse IgG elicited no response according to the I_D–V_G curves shown in Fig. 6(a). This result indicated an electric response specifically produced by the interaction between biotin and streptavidin but not with IgG. In contrast, upon introduction of avidin, which p*I* is around 5, the current increase (Fig. 6(b)) was observed due to the protein's net positive charge. It is interesting to find that an opposite electric response was observed as expected with positively and negatively charged avidin and streptavidin, respectively. The positive charged biomolecule (avidin) produced higher drain current and negative charged biomolecule (streptavidin) made lower drain current, which exactly fit the predicted electric responses from an n-type FET device. To confirm that non-specific interaction between streptavidin/avidin and poly-Si NW FET was not the cause for the change of I_D–V_G curves shown in Fig. 6(a) and (b), controlled experiments using naked poly-Si NW FET were performed (Fig. 6(c)). The results indicated that only specific binding of avidin/streptavidin to the biotin modified on poly-Si NW surface may induce the observed I_D–V_G curve changes (Fig. 6(a) and (b)). The lowest concentration detectable and detection range of streptavidin with biotin-modified poly-Si NW FET was further demonstrated in Fig. 6(d). Continued variations of I_D–V_G curves were observed as streptavidin concentrations increased from 167 fM and saturated at 1.67 nM. The I_D–V_G curve remained constant after saturation even when much higher concentration of streptavidin (167 nM) was added.

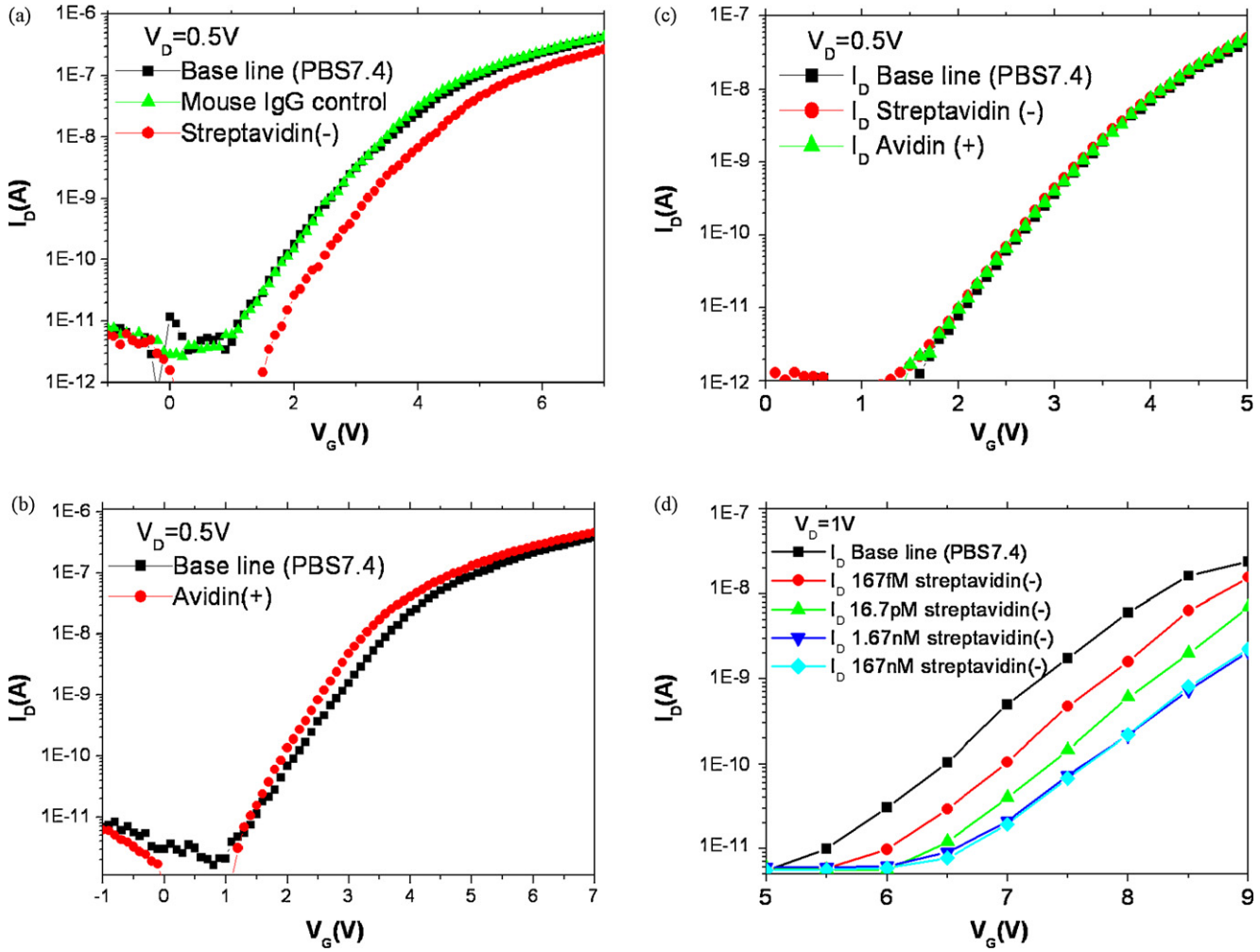

Fig. 6. Electric response of poly-Si NW FET following molecular recognition with streptavidin or avidin. (a) Electric response of biotin-modified poly-Si NW FET following biotin–streptavidin interaction. The I_D–V_G curves were obtained in PBS buffer (10 mM, pH 7.4, black square), and following the addition of mouse IgG (6 pM, green triangle) and addition of streptavidin (16.7 pM, red circle), respectively. (b) Electric response of biotin-modified poly-Si NW FET following biotin–avidin interaction. The interaction of biotin and avidin (1.48 nM, red circle) resulted in an opposite electric response related PBS base line (black square) as compared to that for biotin and streptavidin interaction. (c) I_D–V_G curves of unmodified poly-Si NW FET. The base I_D–V_G curve was obtained in PBS buffer (black square). PBS buffer solution contained avidin (1.48 nM, green triangle) or streptavidin (1.67 nM, red circle) was injected into the channel and the I_D–V_G curves were determined, respectively. (d) Concentration-dependent electric response of biotin-modified poly-Si NW FET following biotin–streptavidin interaction. The I_D–V_G curves were determined as described above by using different concentrations of streptavidin. After the base I_D–V_G curve was obtained in PBS buffer, PBS buffer contained streptavidin at varied concentrations (167 fM, 16.7 pM, 1.67 nM and 167 nM) were injected, respectively, and their I_D–V_G curves were determined. (For interpretation of the references to color in this figure legend, the reader is referred to the web version of the article.)

The result indicates that the poly-Si NW FET was stable in a variety of non-interacting molecules, which is important for its biomedical application. The lowest concentration detectable and detection range were comparable to those using single-Si NW FET (Cui et al., 2001) that required a complex fabrication procedure (Patolsky et al., 2006d).

4. Conclusions

We demonstrated for the first time that a poly-Si NW FET fabricated with a simple and low-cost method was useful for biosensing application. Throughout the fabrication of the poly-Si NW FET, no expensive lithography tools were needed for definition of nanoscale patterns. Our results indicate that fabrication of poly-Si NW FET for sensitive and specific biosensing device can be achieved using commercially available procedures. The poly-Si NW FET should have a great potential as a biosensing device for future application in biomedical diagnosis.

Acknowledgement

The research was financially supported by National Science Council, Taiwan (97-2321-B-009-001 and 96-2120-M-009-001).

References

Besteman, K., Lee, J., Wiertz, F.G.M., Heering, H.A., Dekker, C., 2003. Nano Lett. 3, 727–730.
Campagnolo, C., Meyers, K.J., Ryan, T., Atkinson, R.C., Chen, Y.T., Scanlan, M.J., Ritter, G., Old, L.J., Batt, C.A., 2004. J. Biochem. Biophys. Methods 61, 283–298.
Chen, Y., Wang, X., Hong, M.K., Erramilli, S., Mohanty, P., Rosenberg, C., 2007. Appl. Phys. Lett. 91, 243511.
Cui, Y., Wei, Q., Park, H., Lieber, C.M., 2001. Science 293, 1289–1292.
Duan, X., Huang, Y., Lieber, C.M., 2002. Nano Lett. 2, 487–490.
Duan, X., Niu, C., Sahi, V., Chen, J., Parce, J.W., Empedocles, S., Goldman, J.L., 2003. Nature 425, 274–278.
Hahm, J., Lieber, C.M., 2004. Nano Lett. 4, 51–54.
Hirotsugu, O., Kazuma, M., Kenichi, H., Toshinobu, O., Masahiko, H., Masayoshi, N., 2007. Jpn. J. Appl. Phys. 46, 4693–4697.
Lee, K.N., Jung, S.W., Kim, W.H., Lee, M.H., Shin, K.S., Seong, W.K., 2007. Nanotechnology 18, 445302.

Li, C., Curreli, M., Lin, H., Lei, B., Ishikawa, F.N., Datar, R., Cote, R.J., Thompson, M.E., Zhou, C., 2005. J. Am. Chem. Soc. 127, 12484–12485.
Li, Z., Chen, Y., Li, X., Kamins, T.I., Nauka, K., Williams, R.S., 2004. Nano Lett. 4, 245–247.
Lin, H.C., Lee, M.H., Su, C.J., Huang, T.Y., Lee, C.C., Yang, Y.S., 2005. IEEE Electron Device Lett. 26, 643–644.
Lin, H.C., Su, C.J., 2007. IEEE Trans. Nanotechnol. 6, 206–212.
Lin, H.C., Su, C.J., Hsiao, C.Y., Yang, Y.S., Huang, T.Y., 2007. Appl. Phys. Lett. 91, 202113.
Lu, M.P., Hsiao, C.Y., Lo, P.Y., Wei, J.H., Yang, Y.S., Chen, M.J., 2006. Appl. Phys. Lett. 88, 053114.
McAlpine, M.C., Friedman, R.S., Jin, S., Lin, K.H., Wang, W.U., Lieber, C.M., 2003. Nano Lett. 3, 1531–1535.
Patolsky, F., Zheng, G., Hayden, O., Lakadamyali, M., Zhuang, X., Lieber, C.M., 2004. PNAS 101, 14017–14022.
Patolsky, F., Timko, B.P., Yu, G., Fang, Y., Greytak, A.B., Zheng, G., Lieber, C.M., 2006a. Science 313, 1100–1104.
Patolsky, F., Zheng, G., Lieber, C.M., 2006b. Anal. Chem. 78, 4260–4269.
Patolsky, F., Zheng, G., Lieber, C.M., 2006c. Nanomedicine 1, 51–65.
Patolsky, F., Zheng, G., Lieber, C.M., 2006d. Nat. Protoc. 1, 1711–1724.
Star, A., Tu, E., Niemann, J., Gabriel, J.C.P., Joiner, C.S., Valcke, C., 2006. PNAS 103, 921–926.
Su, C.J., Lin, H.C., Huang, T.Y., 2006. IEEE Electron Device Lett. 27, 582–584.
Su, C.J., Lin, H.C., Tsai, H.H., Hsu, H.H., Wang, T.M., Huang, T.Y., Ni, W.X., 2007. Nanotechnology 18, 215205.
Wang, W.U., Chen, C., Lin, K., Fang, Y., Lieber, C.M., 2005. PNAS 102, 3208–3212.
Wu, G., Datar, R.H., Hansen, K.M., Thundat, T., Cote, R.J., Majumdar, A., 2001. Nat. Biotechnol. 19, 856–860.
Zhang, Y., Heller, A., 2005. Anal. Chem. 77, 7758–7762.
Zheng, G., Patolsky, F., Cui, Y., Wang, W.U., Lieber, C.M., 2005. Nat. Biotechnol. 23, 1294–1301.